PROCEEDINGS. Twenty-Third Workshop on Geothermal Reservoir Engineering
Stanford University. Stanford, California, January 26-28, 1998
SGP-TR-158

INFERRING RELATIVE PERMEABILITY FROM DYNAMIC BOILING EXPERIMENTS

Marilou T. Guerrero[1], Cengiz Satik[1], Stefan Finsterle[2] and Roland Horne[1]

[1]Dept. of Petroleum Engineering
Stanford University
Stanford, CA, USA 94305
marilou@pangea.stanford.edu

[2]Earth Sciences Division
Lawrence Berkeley National Laboratory
Berkeley, CA, USA 94720
finster@lbl.gov

ABSTRACT

This paper describes the estimation of relative permeability and capillary pressure by matching the measurements from a transient experiment to the results of a numerical simulation. The numerical model was constructed in TOUGH2 to simulate results taken from a vertical boiling experiment. Residual water saturation, S_{wr}, residual steam saturation, S_{gr}, pore size distribution index, λ, and gas entry pressure, p_e, were estimated for a Berea sandstone core by forward and inverse calculation using the Brooks-Corey relative permeability and capillary pressure functions.

INTRODUCTION

Relative permeability is important in describing multiphase flow since it contains the information regarding movement of one phase with respect to another. It is given as a function of saturation, interfacial tension, wetting characteristics, and viscosity ratios. So far, relative permeability relations have been based on theoretical methods using field data, and laboratory experiments. Although relative permeability is best determined through laboratory experiments, it is difficult to measure due to capillary forces that introduce nonlinear effects on the pressure and saturation distribution at the core exit (Ambusso, **1996).** In particular, the relative permeability is difficult to measure directly for steam-water flows mainly due to the heterogeneity of the core, equipment or material limitations (i.e. the need to withstand high temperatures and pressures), and inaccuracy of the experimental methods (Satik, **1997).**

Recently, significant improvements were achieved in measuring saturations and collecting data from steam-water flow experiments. These results indicated a linear relationship for steam-water relative permeability (Ambusso, **1996).** In attempting to repeat these results, Satik **(1998)** made a significant improvement in the design of the experimental apparatus. A successful experiment was conducted and steam-water relative permeability was obtained. These recent results suggest a curvilinear relationship that is different from the results obtained by Ambusso **(1996)** (linear relationship).

This paper describes a second approach to estimating the relative permeability by matching data from a boiling experiment with results obtained from numerical simulation. This method provides a way to examine the validity of the relative permeability measurements taken from previous experiments as well as to estimate capillary pressure since the parameters in the relative permeability and capillary functions used (Brooks-Corey functions) are interrelated.

EXPERIMENTAL APPARATUS

In the actual experiment (Fig. 1), a **43** cm long Berea sandstone core with radius **2.54** cm was sealed with epoxy and insulated with ceramic fiber blanket. The core was first saturated with liquid water and then heated at the bottom. Water was allowed to flow out from the top end of the core, which was maintained at atmospheric conditions. The heater was placed at the bottom of the core and insulated to minimize heat loss. During the vertical boiling experiment, temperature, water pressure, and heat flux values were measured at **41** points along the length of the core using thermocouples, pressure transducers, and heat flux sensors; while steam saturation was measured using a CT scanner. The power of the heater was increased nine times from 0.864 mW to 10.42 W. A detailed description of the experiment is given in Satik **(1997).** Table 1 shows the properties of the sandstone and materials used in the experiment.

MODEL

TOUGH2 is a multidimensional numerical model for simulating the transport of water, steam, air, and heat in porous and fractured media (Pruess, **1991).**

ITOUGH2 (Finsterle, 1997) provides inverse modeling capabilities for the TOUGH2 codes and solves the inverse problem by automatic model calibration based on the maximum likelihood approach. In this study, parameters were estimated based on temperature, water pressure, steam saturation, and heat flux for which a corresponding TOUGH2 output was already available, including initial guesses, for the parameters to be estimated.

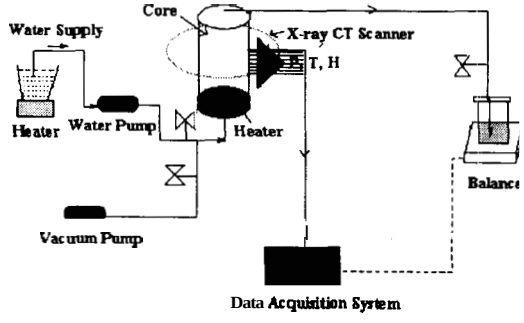

Figure 1. Schematic diagram of the experimental apparatus (from Satik, 1997).

Table 1. Properties of the materials used in the boiling experiment.

Material	ρ kg/m³	k 10^{-13} m²	ϕ %	α W/m-°C	C J/kg-°C
Berea	2163	8.487	22	4.326	858.2
Heater	2200			2.885	
Heater insul.	529			0.125	1046.6
Epoxy	1200			0.577	1046.6
Insulator	192			0.090	104.7

The TOUGH2 simulation grid used is a two-dimensional radial model with 3 rings and 51 layers (Fig. 2). Except for the layers 45-51 (seven bottommost layers), the first (innermost) ring represents the core; the second ring represents the epoxy; and the third ring represents the insulator. The heater is located in the layer **45** in ring 1, and the heater grid block is further refined into five smaller grid blocks. Moreover, the heater insulator is in layers 46-51, rings 1-3. Rings 2-3 in layer **45** represent epoxy and core insulator, respectively. Constant pressure boundary conditions are applied to layer 1 (topmost layer) in ring 1. To simulate a constant pressure boundary, layer 1 grid blocks are assigned a much larger volume than the core layers. All grid blocks from layer 1 to layer 51 in ring 3 and layer 51 in rings 1-2 are attached to a large grid block that is under ambient conditions in order to model heat loss to the surroundings. Since there is no fluid flow in the radial direction, non-zero permeability values are assigned only in the vertical directions.

D BR CTIONS

The modified Brooks relative p functions are g r as:

$$k_{rl} = S_{ek}^{(2-3\lambda)/\lambda} \quad \text{.....} \quad (1)$$

$$k_{rg} = (1 - S_{ek})^2 (1 - S_{ek}^{(2-3\lambda)/\lambda}) \quad \text{.....} \quad (2)$$

The modified Brooks-Corey capillary pressure functions are given as

$$p_c = -p_e \left[\varepsilon / (1 - S_{wr})\right]^{-1/\lambda} - (p_e / \lambda)\left[\varepsilon / (1 - S_{wr})^{(1-\lambda)/\lambda}\right](S_l - S_{wr} - \varepsilon)$$

$$\text{for } S_l < (S_{wr} + \varepsilon) \text{ .....(3)}$$

$$p_c = p^e (S^{ek})^{(2-3\lambda)/\lambda} \quad \text{for } S_l \geq (S_{wr} + \varepsilon) \text{ .....(4)}$$

where

$$S_{ec} = (S_l - S_{wr}) / (1 - S,,) \quad \text{.....} \quad (5)$$

$$S_{ek} = (S_l - S_{wr}) / (1 - S_{wr} - S_{gr}) \quad \text{.....(6)}$$

and S_l is the liquid saturation, S_{wr} is the residual liquid saturation, S_{gr} is the residual gas saturation, λ is the pore size distribution index, and p_e is the gas entry pressure. To prevent the capillary pressure from increasing to infinity as the effective saturation approaches zero, a linear function is used for $S_l < (S_{lr} + \varepsilon)$, where ε is a small number (Equation 3).

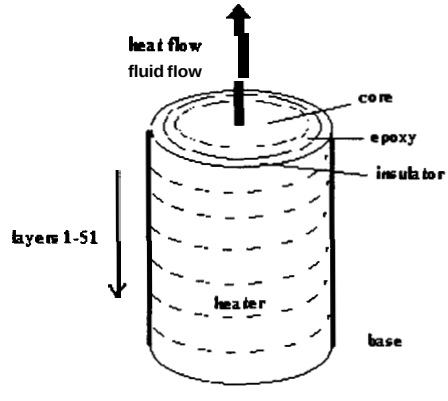

Figure 2. Schematic diagram of the 3x51 TOUGH2 model.

PARAMETER ESTIMATION

Forward Calculation

To avoid time-consuming inverse calculations, forward runs were done first to roughly match the experimental data (temperature, pressure, steam

saturation, and heat flux) with simulated results. The sensitivity of the system response to the parameters under investigation (S_{wr}, S_{gr}, λ, and p_c) was determined. However, since these are parameters related to two-phase flow conditions, the system response, as calculated by TOUGH2, showed sensitivity only when there were steam and water present. In the experiment, two-phase conditions were observed after 120 hours from the start of the experiment.

Results of the sensitivity analysis showed that temperature, pressure, and steam saturation were higher at lower **S,.** Conversely, temperature, pressure, and steam saturation were lower at higher S_{wr}. At the same water saturation value, the capillary pressure decreased as **S,** was increased. Moreover, the temperature, pressure, and steam saturation were higher at lower S_{gr} while they were lower at higher S_{gr}. The capillary pressure did not change with **S,,** since it is not a function of S_{gr}. At lower values of λ, the temperature, pressure, and steam saturation were lower than at higher values of λ. The relative permeability of water became more concave upwards at lower λ, then became linear at a certain value, after which it became more convex downwards. The capillary pressure increased as λ was decreased. Furthermore, the temperature, pressure, and steam saturation were higher at smaller values of p_c due to the lower capillary pressure required to displace the water by steam.

By trial-and-error a rough fit to the experimental data was obtained at the following values: S_{wr}=0.2, S_{gr}=0.2, λ=0.5, p_c=500 Pa, and ε=0.05. In all the plots given in this paper, T1, P1, Sst1, and HF1 are temperature, pressure, saturation, and heat flux measured at 1 cm from the heater, respectively. T2, P2, Sst2, and HF2 are measured at 2 cm from the heater. T3, P3, Sst3, and HF3 are measured at 3 cm from the heater. Finally, T4, P4, Sst4, and HF4 are measured at 4 cm from the heater.

The measured and simulated temperature data consistently differ by 6-12 "**C** from T1 to T4 (Figs. 3a and 3b). The simulated pressures mimic the observed data from P1 to P4 (Figs. 4a and 4b), although the differences are still large considering that the gauge pressure measurement range is only –28,000 Pa. The maximum difference between the measured and calculated pressure values is –6000 Pa (Fig. 4b). In terms of steam saturation, the fit is slightly poor since there are only three sets of steam saturation data to compare the simulated results (Figs. 5a and 5h). To generate data at the specified observation times, TOUGH2 interpolated between the two measured data points. The real data and the interpolated data points were used to calibrate the model, which involved comparing simulated results with experimental data and minimizing the weighted difference between them. However, the interpolated steam saturation data are not shown on Figures 5a and 5b. The observed and simulated heat flux data have a good fit at all measurement points except at HF1, where the maximum difference between the observed and calculated data is –225 W/m^2 (Figs. 6a and 6b). Relative permeability (Brooks-Corey) and capillary pressure (Brooks-Corey) curves used to obtain these results are given in Figures 7 and 8, respectively.

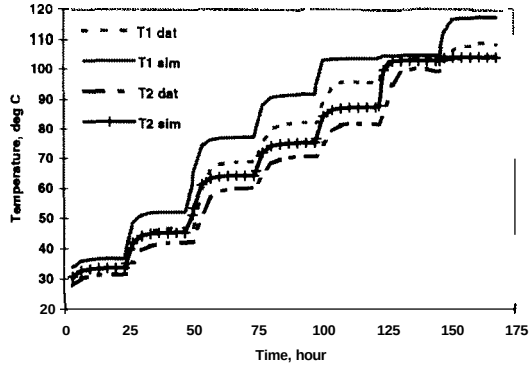

Figure 3a. Observed and simulated temperature data at T1 and T2 generated from initial guesses.

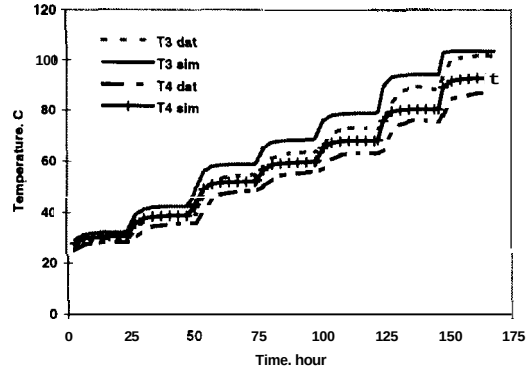

Figure 3b. Observed and simulated temperature data at T3 and T4 generated from initial guesses.

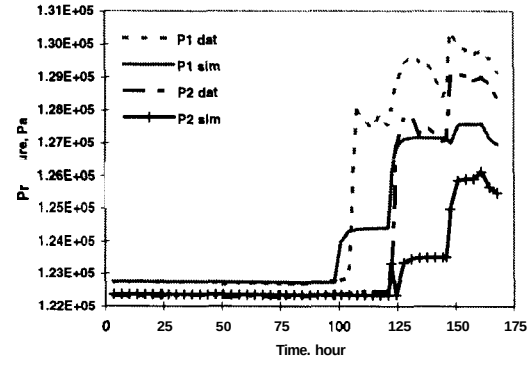

Figure 4a. Observed and simulated pressure data at PI and P2 generated from initial guesses

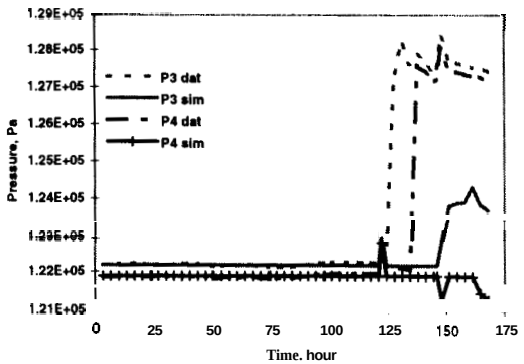

Figure 4b. Observed and simulated pressure data at P3 and P4 generated from initial guesses

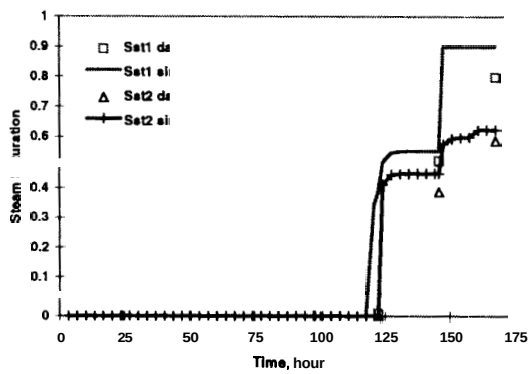

Figure 5a. Observed and simulated steam saturation at Sstl and Sst2 generated from initial guesses.

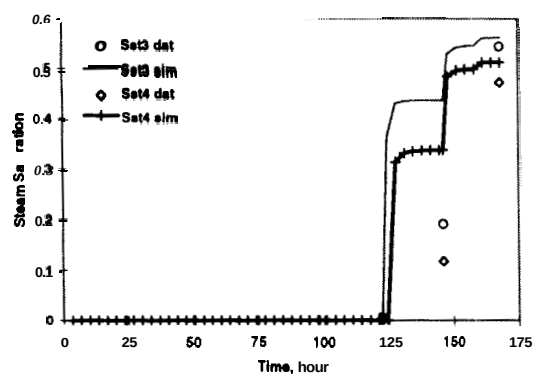

Figure 5b. Observed and simulated steam saturation at Sst3 and Sst4 generated from initial guesses.

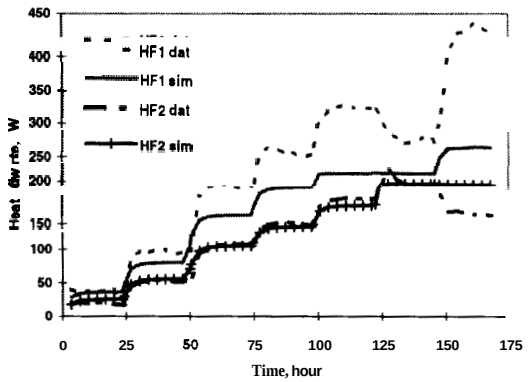

Figure 6a. Observed and simulated heat flux data at HFI and HF2 generated from initial guesses.

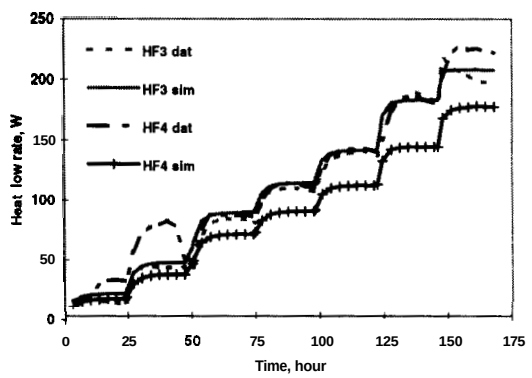

Figure 6b. Observed and simulated heat flux data at HF3 and HF4 generated from initial guesses.

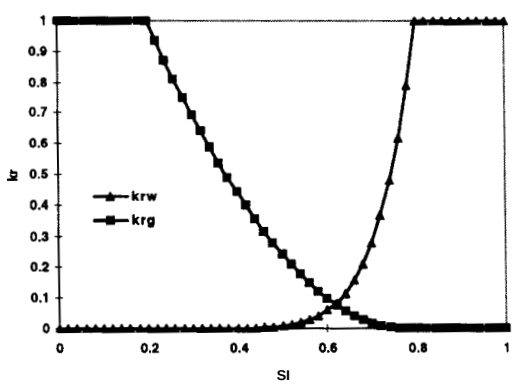

Figure 7. Brooks-Corey relative permeability curves at S_{wr}=0.2, S_{gr}=0.2, and λ=0.50, p_t=500 Pa.

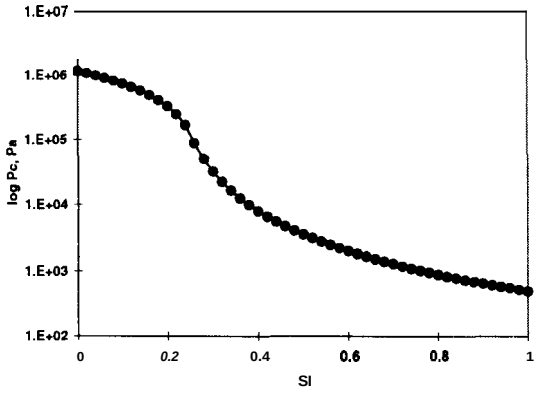

Figure 8. Modijied Brooks-Corey capillary pressure curve at S_{wr}=0.2, S_{gr}=0.2, λ=0.5, p_e=500 Pa and ε=0.05.

Inverse Calculation

Higher accuracy of the model prediction can be achieved by a combined inversion of all available data since data types contribute to parameter estimation in different degrees during the calibration phase, when simulated data are compared with real data and the weighted difference between them is minimized (Finsterle et al, 1997). The model was calibrated against temperature, pressure, steam saturation, and heat flux (Table 2) to estimate S_{wr}, S_{gr}, h, p_e, thermal conductivity of sandstone, σ_s, thermal conductivity of insulator, σ_i, thermal conductivity of heater insulator (or the base), σ_b, and absolute permeability of sandstone, k. The standard deviation values given in Table 2 reflect the uncertainty associated with the measurement errors. Table 3 shows a summary of the estimated parameter set.

The parameter estimates remarkably improve the temperature match, and to some extent the pressure match (Figs. 9a, 9b, 10a, and 10b). Based on the few measured steam saturation data points available, the fit is also improved by using estimates obtained from inverse calculation (Figs. 11a and 11b). On the other hand, there is no considerable improvement in the heat flux match (Figs. 12a and 12b). The Brooks-Corey relative permeability and pressure capillary curves corresponding to the estimated values of S_{wr}, S_{gr}, λ, and p_e are shown in Figures 13 and 14, respectively. Figure 13 suggests that the core is strongly water-wet as indicated by the position of the intersection of the relative permeability curves.

The covariance and correlation matrices are given in Table 4, where the diagonal elements give the square of the standard deviation of the parameter estimate, σ_p. σ_p takes into account the uncertainty of the parameter itself and the influence from correlated parameters. In Table 5, the conditional standard deviation, σ_p* reflects the uncertainty of one parameter if all the other parameters are known. Hence, σ_p*/σ_p (column 3) is a measure of how independently a parameter can be estimated. A value close to one denotes an independent estimate, while a small value denotes strong correlation to other uncertain parameters. The total parameter sensitivity (column 4) is the sum of the absolute values of the sensitivity coefficients, weighted by the inverse of individual measurement errors and scaled by a parameter variation (Finsterle et al, 1997).

As shown in Table 5, σ_i and σ_b are the most sensitive parameters. Except for σ_b, all parameters cannot be determined independently because they are strongly correlated to one or more of the other parameters (Table 3). Moreover, the relatively large standard deviation of the estimated values of λ and p_e are due to the fact that they are closely related as indicated by their comparatively high correlation coefficient (Table 3). Also, λ is correlated to p_e since the capillary pressure is dependent on both λ and p_e (Equations 3 and 4).

Table 6 gives the statistical parameters related to the residuals. Comparing the total sensitivity (column 2) of the different observation types, accurate measurements of temperature, pressure, and steam saturation are sufficient to solve the inverse problem, i.e. heat flux data are much less sensitive. The standard deviation values of the final residual (column 3) are of the same order of magnitude as the measurement errors (Table 2) indicating that there are no significant systematic errors present. Lastly, the contribution of each observation type to the final value of the objective function (COF) is relatively evenly distributed suggesting that the choice of weighting factor is reasonable.

CONCLUSION

It has been demonstrated that it is possible to infer relative permeability using transient experimental data by inverse calculation. Other relative permeability and capillary pressure functions (e.g. van Genuchten) will be used to potentially improve the fit.

This work was funded by the U.S. Department of Energy under grant number DE-FG07-95ID13370

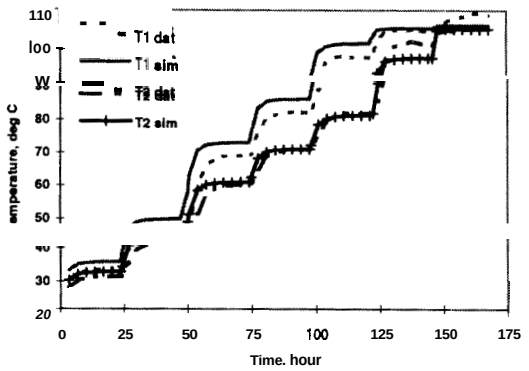

Figure 9a. Observed and simulated temperature data at T1 and T2 generated from estimated values.

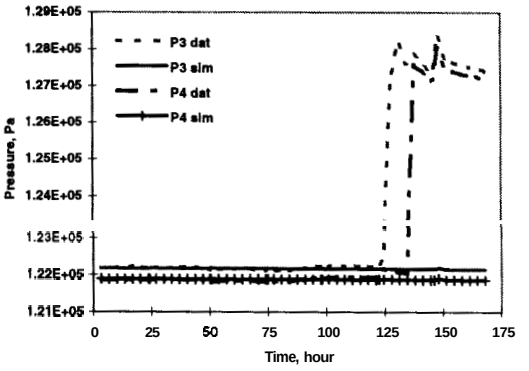

Figure 1Ob. Observed and simulated pressure data at P3 and P4 generated from estimated values.

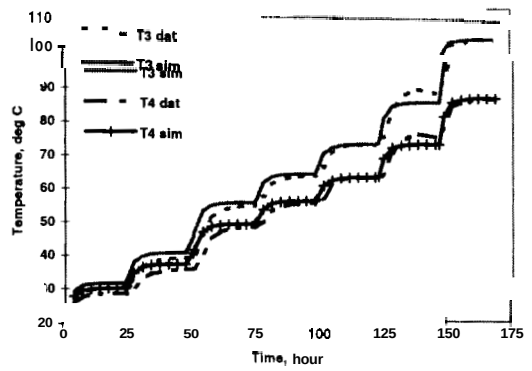

Figure 9b. Observed and simulated temperature data at T3 and T4 generated from estimated values.

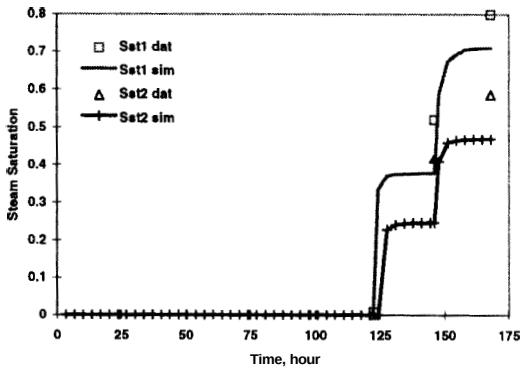

Figure 11a. Observed and simulated steam saturation data at Sstl and Sst2 generated from estimated values.

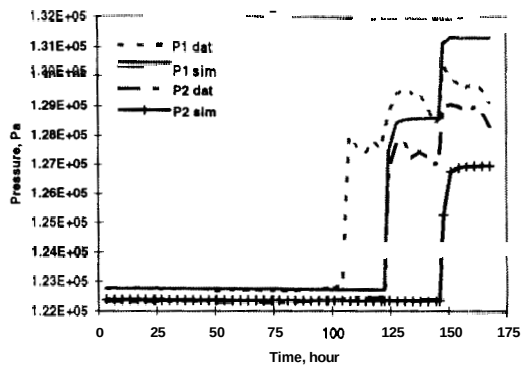

Figure 10a. Observed and simulated pressure data at P1 and P2 generated from estimated values.

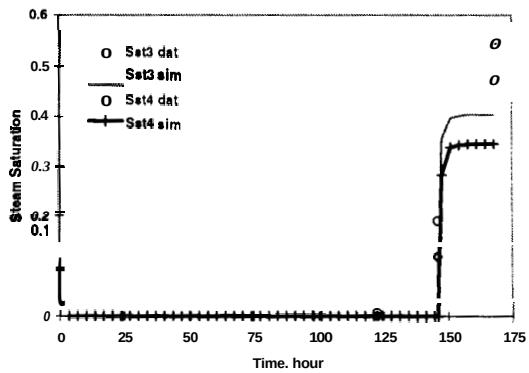

Figure 11b. Observed and simulated steam saturation data at Sst3 and Sst4 generated from estimated values.

Table 2. Observation used for model calibration

Data Type	Standard Deviation
Temperature	1°C
Pressure	1000 Pa
Steam Saturation	0.01
Heat Flux	20 W/m²

Table 3. Parameter initial guesses and estimated values.

Parameter	Initial Guess	Best Estimate	Difference
σ_s, W/m-C	4.326	4.299	-0.027
σ_l, W/m-C	0.090	0.095	0.005
σ_b, W/m-C	0.125	0.172	0.047
Log k, m^2	-12.07	-12.31	-0.24
S_{wr}	0.200	0.209	0.009
S_{gr}	0.200	0.065	-0.135
λ	0.500	0.343	0.157
Log p_e, Pa	2.70	2.98	-0.28

Table 4. Variance-covariance matrix (diagonal and lower triangle) and correlation matrix (upper triangle).

	σ_s	σ_l	σ_b	log k
σ_s	6.3E-3	-0.97	0.12	-8 6E-2
σ_l	-2.7E-4	1.2E-5	-0.20	0.19
σ_b	1.5E-6	-1.1E-7	2.5E-8	0.11
log k	-2.7E-4	2.7E-5	7.2E-7	1.6E-3
S_{wr}	5.1E-4	-2.2E-5	4.1E-7	-5.6E-4
S_{gr}	0.37	-0.17	0.28	-5.2E-6
λ	7.1E-4	-2.6E-5	5.2E-7	-1.2E-3
log p_e	3.2E-4	-2.0E-5	-1.0E-6	-2.9E-3

	S_{wr}	S_{gr}	λ	log p_e
σ_s	0.19	0.21	0.15	3.7E-2
σ_l	-0.18	-0.22	-0.12	-5.4E-2
σ_b	7.5E-2	8.0E-2	5.4E-2	-6.0E-2
log k	-0.41	-5.9E-3	-0.50	-0.68
S_{wr}	1.2E-3	0.51	0.74	0.44
S_{gr}	3.8E-4	4.7E-3	-0.11	-0.45
λ	1.5E-3	-1.4E-4	3.7E-3	0.88
log p_e	1.6E-3	-1.0E-3	5.7E-3	1.1E-2

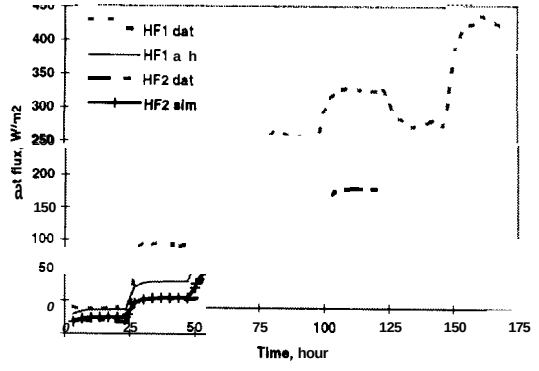

Figure 12a. Observed and simulated heat flux data at HF1 and HF2 generated from estimated values.

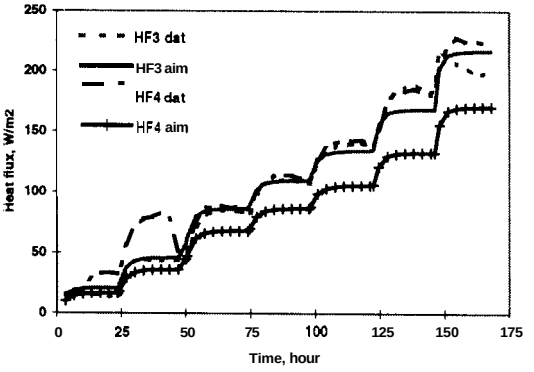

*Figure 12b. Observed and simulated heat flux data at **HF3** and **HF4** generated from estimated values*

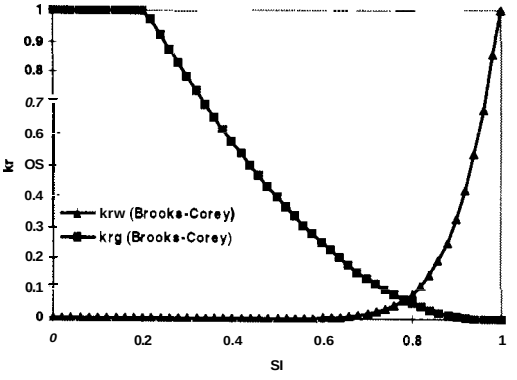

Figure 13. Brooks-Corey relative permeability curves at S_{wr}=0.209, S_{gr}=0.065, and λ=0.343.

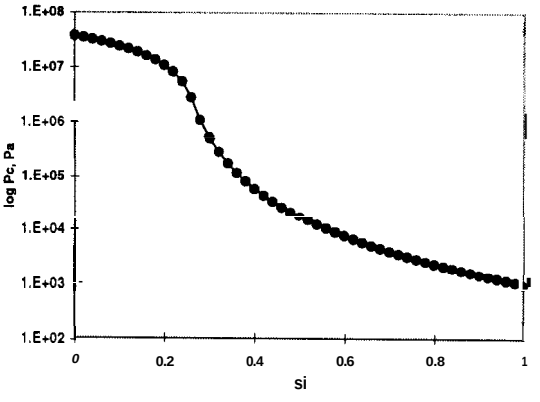

*Figure **14.** Modified Brooks-Corey capillary pressure curve at S_{wr}=0.209, S_{gr}=0.065, λ=0.343, p_e=973 Pa, and ε=0.05*

Table 5. Statistical measures and parameter sensitivity.

Parameter	σ_{p}	$\sigma_{p}^{*}/\sigma_{p}$	Parameter Sensitivity
σ_s	0.079	0.151	1482
σ_i	0.0035	0.151	35302
σ_r	0.00016	0.675	288850
log k	0.04	0.142	2112
S	0.0346	0.258	1989
S_{or}	0.022	0.143	3522
λ	0.061	0.062	4075
log p,	0.106	0.048	2428

Table 6. Total sensitivity of observation, standard deviation of residuals, and contribution to the objective function (COF).

Observation	Sensitivity	Std Dev	COF %
Temperature	1415.8	2.2	22.44
Pressure	1271.3	1460	11.27
Saturation	3164.4	0.01	43.10
Heat flux	265.5	29.3	22.93

REFERENCES

[1] W.J. Ambusso, 1996. Experimental Determination of Steam-Water Relative Permeability Relations. MS Thesis, Stanford University, Stanford. Calif.

[2] R.H. Brooks and A.T. Corey, 1964. Hydraulic Properties of Porous Media, Colorado State University, Hydro paper No.5.

[3] A.T. Corey, 1954. The Interrelations Between Gas and Oil Relative Permeabilities, Producers Monthly Vol. 19 pp 38-41.

[4] S. Finsterle, 1997. ITOUGH2 Command References Version 3.1, Lawrence Berkeley National Laboratory, Berkeley, Calif.

[5] S. Finsterle, K. Pruess, D.P. Bullivant, and M.J. O'Sullivan, 1997. Application of Inverse Modeling to Geothermal Reservoir Simulation, Proc. of 22nd Workshop on Geothermal Reservoir Engineering, Stanford, Calif.

[6] K. Pruess, 1987. TOUGH User's Guide, Lawrence Berkeley National Laboratory, Berkeley, Calif.

[7] K. Pruess, 1991. TOUGH2-A General Purpose Numerical Simulator for Multiphase Fluid and Heat Flow, Report LBL-29400, Lawrence Berkeley National Laboratory, Berkeley, Calif.

[8] C. Satik (1997), A Study of Boiling in Porous Media, Proc. 19* New Zealand Geothermal Workshop, Auckland, NZ.

[9] C. Satik (1998), A Measurement of Steam-Water Relative Permeability, Proc. of 23rd Workshop on Geothermal Reservoir Engineering, Stanford, Calif.

[10] M.L. Sorey, M.A. Grant and E. Bradford, 1980. Nonlinear Effects in Two Phase Flow to Wells in Geothermal Reservoirs. Water Resources Research, Vol. 16 No. 4, pp 767-777.